Published article:

The role of moist convection in the West African monsoon system: Insights from continental-scale convection-permitting simulations

John H. Marsham,[1,2] Nick S. Dixon,[2] Luis Garcia-Carreras,[2] Grenville M. S. Lister,[1,3] Douglas J. Parker,[2] Peter Knippertz,[2] and Cathryn E. Birch[2]

[1]   Predicting the West African monsoon (WAM) remains a major challenge for weather and climate models. We compare multiday continental-scale simulations of the WAM that explicitly resolve moist convection with simulations which parameterize convection. Simulations with the same grid spacing but differing representations of convection isolate the impact of the representation of convection. The more realistic explicit convection gives greater latent and radiative heating farther north, with latent heating later in the day. This weakens the Sahel-Sahara pressure gradient and the monsoon flow, delaying its diurnal cycle and changing interactions between the monsoon and boundary layer convection. In explicit runs, cold storm outflows provide a significant component of the monsoon flux. In an operational global model, biases resemble those in our parameterized case. Improved parameterizations of convection that better capture storm structures, their diurnal cycle, and rainfall intensities will therefore substantially improve predictions of the WAM and coupled aspects of the Earth system. Citation: Marsham, J. H., N. Dixon, L. Garcia-Carreras, G. M. S. Lister, D. J. Parker, P. Knippertz, and C. Birch (2013), The role of moist convection in the West African monsoon system: Insights from continental-scale convection-permitting simulations, Geophys. Res. Lett., 40, 1843–1849, doi:10.1002/grl.50347.

1. Introduction

[2]   The West African monsoon (WAM) brings seasonal rains to the Sahel and is therefore essential to the livelihoods of millions. The monsoon flow is driven by the low-level pressure gradient toward the Saharan heat low. In common with most tropical continental regions, there are substantial errors in the WAM region in global weather and climate models [*Thorncroft et al.*, 2003; *Augusti-Panareda et al.*, 2010; *Xue et al.*, 2010; *Bock et al.*, 2011]. For example, many analyses unrealistically show West Africa as a moisture source rather than a sink during the summer [*Meynadier et al.*, 2010], and models generally do not make accurate seasonal predictions in the Sahel [*Philippon et al.*, 2010]. There are significant intermodel variations in climate projections of the WAM [*Solomon et al.*, 2007; *Cook*, 2008; *Biasutti and Sobel*, 2009; *Druyan*, 2011], making it difficult to predict the impacts of climate change and to develop adaption strategies.

[3]   The representation of moist convection is a particular problem for representing the WAM in models [e.g., *Bock et al.*, 2011; *Pohl and Douville*, 2011]. Convective clouds are parameterized in global models, as they cannot be resolved, and this results in a poor representation of many aspects of the convection: parameterizations tend to produce too much light rainfall and too little intense rainfall, with the peak in rainfall too early in the day [*Randall et al.*, 2003; *Yang and Slingo*, 2005; *Stephens et al.*, 2010; *Dirmeyer et al.*, 2012]. They also struggle to capture the processes whereby convection organizes on scales of hundreds of kilometers forming mesoscale convective systems (MCSs), which can persist long after the daytime heating has ended [e.g., *Davis et al.*, 2003]. In the Sahel, MCSs bring 90% of the rainfall [*Mathon et al.*, 2002], and it is therefore unsurprising that global models exhibit large precipitation errors in this region.

[4]   It has been recognized that the WAM involves substantial interactions and exchanges between the organized moist convection and the continental-scale monsoon [*Redelsperger et al.*, 2002; *Diongue et al.*, 2002; *Zhang et al.*, 2008], but it has not been possible to assess the overall impact of convection: quantifying the interaction of convective storms with the monsoon circulation has been hampered by the inability of a single model to resolve the convection explicitly on a domain that includes the entire WAM region over many days. In this paper, we compare multiday, continental-scale simulations which resolve convection with those in which convection is parameterized. By comparing simulations with the same grid spacing, we isolate the impact of the representation of moist convection, which reveals the interactions between convection and the WAM.

2. Method

[5]   Within the *Cascade* project, simulations using the UK Met Office Unified Model (UM) were run with grid spacings of 4 and 12 km for 25 July to 4 August 2006 (the simulation setups are given in Text S1 in the auxiliary material) [*Pearson et al.*, 2010]. The runs used a standard setup (the MetUM) [*Lean et al.*, 2008], with parameterized deep convection using a CAPE (Convective Available Potential Energy) closure at 12 km ("12kmParam") and very little parameterized convection ("explicit" convection) at 4 km ("4kmExp"). A second 12 km simulation was run with explicit convection ("12kmExp"). A 12 km grid spacing is very large for explicit convection: it is far from resolving individual cumulonimbus updrafts but can give a reasonable simulation of squall lines (features which dominate Sahelian precipitation) [*Mathon et al.*, 2002], although heat transports,

---

[1]National Centre for Atmospheric Science, UK.
[2]School of Earth and Environment, University of Leeds, Leeds, UK.
[3]Department of Meteorology, University of Reading, Reading, UK.

Corresponding author: J. H. Marsham, School of Earth and Environment, University of Leeds, Leeds LS6 4LG, UK. (J.Marsham@leeds.ac.uk)

rainfall rates, and circulations can be overpredicted and cold pools can be too weak and develop too slowly [*Weisman et al.*, 1997; *Marsham et al.*, 2011]. *Pearson et al.* [2010] showed that the 4 km model generates a more realistic timing of deep convection than the 12 km parameterized run, with a more realistic upscale growth of convection.

[6] In the original *Cascade* simulations [e.g., *Marsham et al.*, 2011], the boundary layer (BL) scheme had a capping lid in parameterized runs. In order to have two runs that are identical apart from the representation of convection, we performed a new 12 km parameterized run with an uncapped BL ("12kmParam"). Our analysis uses this 12kmParam run with 12kmExp to isolate the impact of the representation of convection: the use of explicit convection at 12 km grid spacing is justified by a comparison of the 12kmExp run with observations and the standard 4kmExp setup (Section 3.1).

[7] In addition, we use operational UM global forecasts and analyses, rain rates from the Tropical Rainfall Measuring Mission (TRMM) [*Kummerow et al.*, 2000], and the Climate Prediction Centre (CPC) Morphing technique (CMORPH) [*Joyce et al.*, 2004], with surface pressure data from SYNOP observations and the Atmospheric Radiation Measurement mobile facility deployed during the African Monsoon Multi-disciplinary Analyses campaign (Text S1).

3. Results

3.1. Simulated and Observed Moist Convection

[8] Figure 1a shows that the diurnal cycles in 12kmExp and 4kmExp are similar to each other and markedly different from that in 12kmParam. The timing of the diurnal maximum in precipitation in the explicit runs at 18 UTC is similar to that observed, although the models have almost twice as much precipitation at this time, decreasing to a more realistic rate by 00 UTC. The maximum precipitation in 12kmParam occurs approximately 6 h too early, a common feature of parameterized convection [*Yang and Slingo*, 2005; *Stephens et al.*, 2010; *Dirmeyer et al.*, 2012].

[9] Figure 1b shows that the latitudinal distribution of rainfall is much more strongly dependent on the representation of convection than on resolution: the two explicit runs (4kmExp and 12kmExp) are much more similar than the two 12 km runs (12kmParam and 12kmExp). The latitudinal distribution in the explicit runs is closer to observations than that in 12kmParam, with a bimodal distribution in 12kmExp similar to that observed: over 10°W to 10°E and 5°N to 25°N, the rainfall in 12kmExp is 26% and 22% larger than the observations from TRMM and CMORPH, respectively, and 89% larger than that in 12kmParam, which has 35% less rain than that observed. The most significant differences between models occur between 9°N and 18°N, toward the northern side of the observed rain maximum, where MCSs are dominant [*Mathon et al.*, 2002]. The maximum at 9.5°N is overestimated and 1° or 2° too far north in the explicit runs and largely absent in 12kmParam. From 9°N to 18°N, 12kmParam underestimates rainfall by a factor of approximately 2. The 12kmExp is close to observations from 12°N to 18°N but has 1.5 times as much rain from 9°N to 12°N. The southward bias of the precipitation in 12kmParam is a common feature of many models and analyses [*Meynadier et al.*, 2010]: the 12kmExp rainfall corrects and even overcompensates for this bias. The 12kmParam gives too uniform a distribution of rain, while the explicit models overpredict maximum rainfall accumulations (Figure S2 in the auxiliary material; consistent with *Stephens et al.* [2010] and *Weisman et al.* [1997]).

[10] Although perhaps surprising, the similarity of the convection in 12kmExp with 4kmExp is consistent with previous studies using other models [*Dirmeyer et al.*, 2012]. A more detailed evaluation of this model by *Pearson et al.* (2013) shows that 12kmExp actually gives a better diurnal cycle of cloud system evolution than 4kmExp. Although both the parameterized and explicit representations of convection exhibit biases relative to observations, the explicit runs show substantial improvements in the amount, latitudinal distribution, and diurnal cycle of rainfall relative to the parameterized run. Despite the remaining biases in the explicit runs relative to observations, they offer an opportunity to evaluate the sensitivity of the whole WAM system to these improvements in the convective distribution. Furthermore, the similarity between 12kmExp, 4kmExp, and observations, compared with the standard 12kmParam run, allows us, in the next section, to isolate the effects of the representation of convection from the effects of model resolution, by comparing 12kmParam and 12kmExp.

3.2. Impacts of the Representation of Convection on the Simulated Monsoon

3.2.1. Impacts on the Mean State

[11] The later timing of the explicit moist convection decreases daytime cloud cover and increases nocturnal cloud cover, significantly improving the diurnal cycle of cloudiness, and outgoing longwave radiation, compared with observations [*Pearson et al.*, 2010; *Pearson et al.*, 2013]. This gives greater net radiative heating at the surface in 12kmExp compared with 12kmParam, especially in the Sahel (Figure 1c). The net surface radiative balance is dominated by the increased shortwave (see Figure 2a), giving $14 \, \mathrm{W \, m^{-2}}$ greater net surface heating over 10°W to 10°E and 5°N to 25°N in 12kmExp. Over the same area, there is 2.5 mm/d more rain in 12kmExp than in 12kmParam. The rain is generated by moist convection, which warms the upper levels and cools the low levels by rainfall evaporation, with net heating since all rain does not evaporate. The 2.5 mm/day amount of rain corresponds to an additional heating of around $64 \, \mathrm{W \, m^{-2}}$, which is 4.6 times the difference in radiative heating.

[12] The heating affects the low-level pressure gradient south of the Sahara, which drives the monsoon flow. Figure 1d shows that the height of the 950 hPa surface is lower in 12kmExp than in 12kmParam, particularly over the Sahel, leading to a weaker pressure gradient in 12kmExp. This is caused by the greater heating from greater rainfall and net surface radiation over the Sahel in 12kmExp (Figures 1b and 1c). As a result, 12kmExp is warmer than 12kmParam between 10°N and 15°N at 500 to 200 hPa and below 800 hPa (Figure 1e). Through the thickness relationship for a hydrostatic atmosphere, the warmer air column in 12kmExp causes a lower surface pressure. This effect on the mean 950 hPa geopotential height from explicit moist convection forms within 1 day (Figure S3 in the auxiliary material) and is larger than the effect of decreasing horizontal grid spacing from 12 to 4 km (Figure S4 in the auxiliary material). The northward shift in the African easterly jet [*Schubert et al.*, 1991; *Thorncroft et al.*, 1999] in 12kmExp (Figure S5 in the auxiliary material) is consistent with Figure 1e (Text S3 in the auxiliary material).
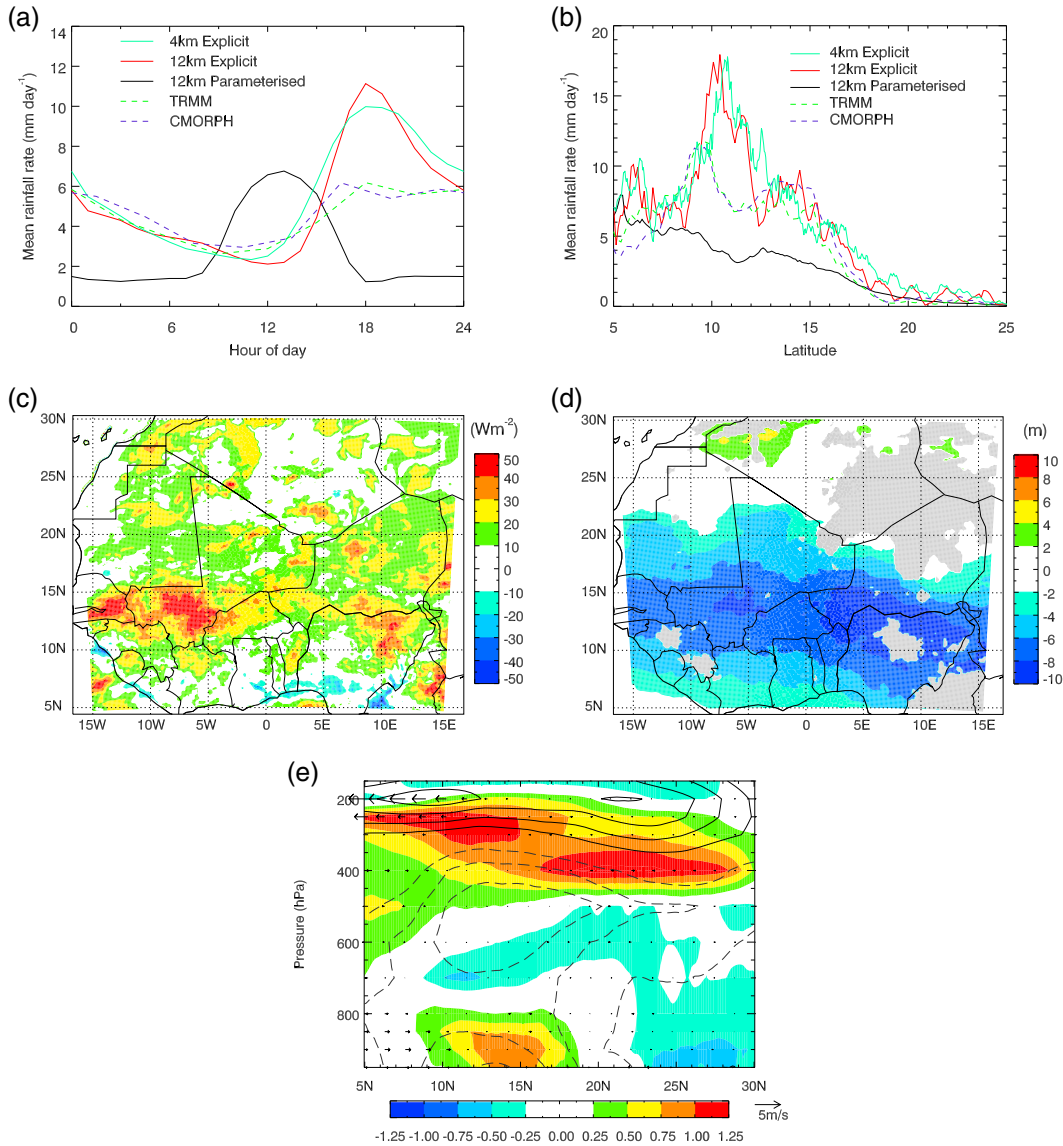
Figure 1. (a) Diurnal cycle in rain in 12kmParam, 12kmExp, and 4kmExp and from TRMM and CMORPH retrievals, averaged over 5°N to 25°N and 10°W to 10°E. (b) Mean latitudinal distributions of rain for the same runs and the same longitudes. The 12kmExp-12kmParam difference in (c) net surface radiation, (d) 950 hPa geopotential height (grey shows orography intersecting the 950 hPa surface), and (e) vertical cross section of geopotential height (lines with 2 m spacing; the dashed lines are negative) and potential temperature (colors; K) over 10°E to 10°W.

### 3.2.2. Impacts on the Diurnal Cycle of the Monsoon

[13]   The difference in the diurnal cycle in moist convection (Figure 1a) drives a diurnal difference in radiation (Figure 2a), with approximately $60 \, \mathrm{W \, m^{-2}}$ greater net heating at midday in 12kmExp but similar longwave cooling at night. In combination, the different diurnal cycles in condensational and radiative heating lead to differences in the north-south pressure difference that drives the monsoon winds (Figure 2b).

[14]   Figure 2b shows that the diurnal cycle of the Sahel-Sahara pressure difference is consistent with the different timing of the rain in the two runs (Figure 1a). Both runs build a stronger (more negative) pressure gradient from the time of their maximum rainfall (18 UTC for 12kmExp and 15 UTC for 12kmParam) to 00 UTC. From 00 to 12 UTC, this pressure gradient dissipates in both runs, with little change in the gradient between 12 and 15 UTC in the 12kmExp run. Overall, the 12kmExp run therefore has a shorter building phase and a longer dissipation phase (see Text S4 in the auxiliary material for more details). In the dissipation phase, the nocturnal meridional flow responds to the pressure gradient (Figure 2b), while during the day, dry convection suppresses the winds [*Parker et al.*, 2005]. In the parameterized run, the dry convection is centered on the time of the minimum pressure gradient and the winds lag the gradient, giving an ellipsoidal shape in Figure 2c (also Figure S6 in the auxiliary material). In 12kmExp, the dry convection occurs 6 h before the minimum pressure gradient, giving a "figure-of-eight" shape (clearest at 06 to 15 UTC, where the winds decline for an almost constant pressure gradient).

3.2.3. The Role of Cold Pool Outflows From Moist Convection

[15]   Cold pools, generated by evaporation of precipitation, are an important component of MCSs and have been observed to ventilate the Sahara [*Flamant et al.*, 2007; *Marsham et al.*,
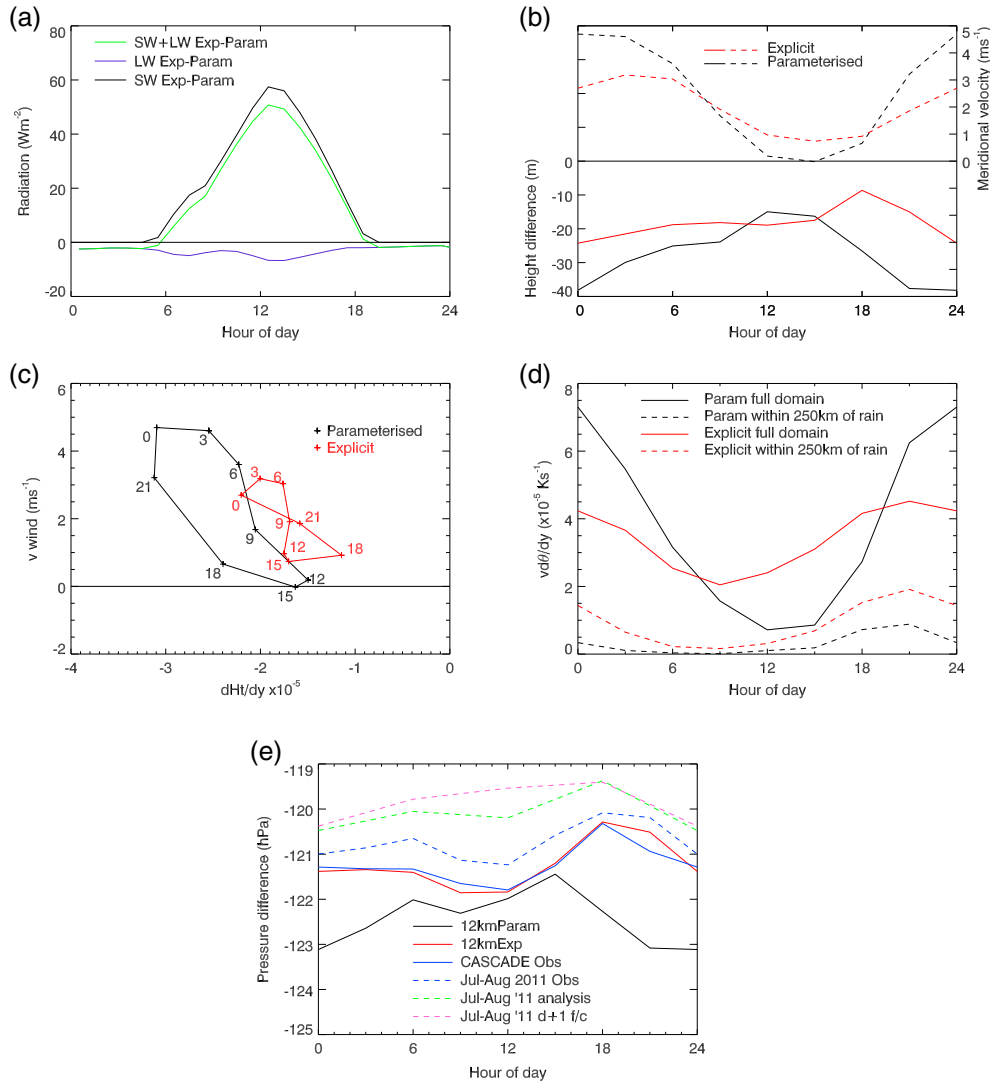
Figure 2. Differences in the diurnal cycle between 12kmParam and 12kmExp: (a) surface radiation (12°N to 24°N and 10°W to 10°E); (b) 950 hPa geopotential height difference between the Sahel and the Sahara (12°N to 24°N) and meridional winds (dashed) over 10°W to 10°E; (c) 950 hPa geopotential gradient between the Sahel and the Sahara and meridional winds. (d) Total cooling by meridional advection ($v \cdot d\theta/dy$) over 13°N to 25°N and 10°W to 8°E (solid lines) and over this domain and within 250 km of rain (dashed lines); (e) pressure difference between Tamanrasset (22.8°N 5.5°E) and Niamey (13.5°N 2.1°E): observed (*Cascade* period in 2006 and in July and August 2011), in *Cascade* runs (2006), and in UM analyses and forecasts (July and August 2011; 6 hourly with $T+6$ to $T+24$). Offsets have been applied to account for the height differences between the surface stations and equivalent model grid boxes.

2008; *Emmel et al.*, 2010] but are very poorly captured by parameterized convection [*Davis et al.*, 2003; *Knippertz et al.*, 2009; *Marsham et al.*, 2011]. As a result, cold pools are responsible for a significant fraction of global UM forecast bias in the Sahara [*Garcia-Carreras et al.*, 2013]. In 12kmExp, the meridional eddy heat fluxes associated with rainfall transport cold air northward and southward, with 6 times more northward transport (Figure 3a). The meridional fluxes lead to advective cooling (Figure 3b). The diurnal cycle in cooling by meridional advection is weaker in 12kmExp than in 12kmParam (Figure 2d), consistent with its weaker cycle in winds (Figure 2b). The cooling and winds peak at 00 UTC in 12kmParam, whereas cooling peaks at 21 UTC in 12kmExp, when cold pools are most active, 6 h before its peak in winds: although this effect may be underestimated in 12kmExp, since cold pool winds in 12kmExp lag those in

4kmExp by around 3 h, consistent with the coarser grid spacings [*Weisman et al.*, 1997; *Marsham et al.*, 2011]. Approximately 30% of the cooling occurs within 250 km of rain in 12kmExp, but this is only 10% in 12kmParam, where the cold pools are essentially missing (Figures 2d, 3c, and 3d). The cooling from the cold pools missing in 12kmParam is replaced by stronger synoptic scale winds (Figure 2b), leading to a compensation of errors.

3.2.4. Implications for the Global Unified Model

[16] The parameterization of convection is a source of error in all global models. The global operational UM is very similar in its formulation to the regional MetUM used in *Cascade*, and so we expect fingerprints of the errors from the parameterization of convection in this model, although these will be combined with other sources of error. Within 1 day, meridional pressure gradients in UM forecasts
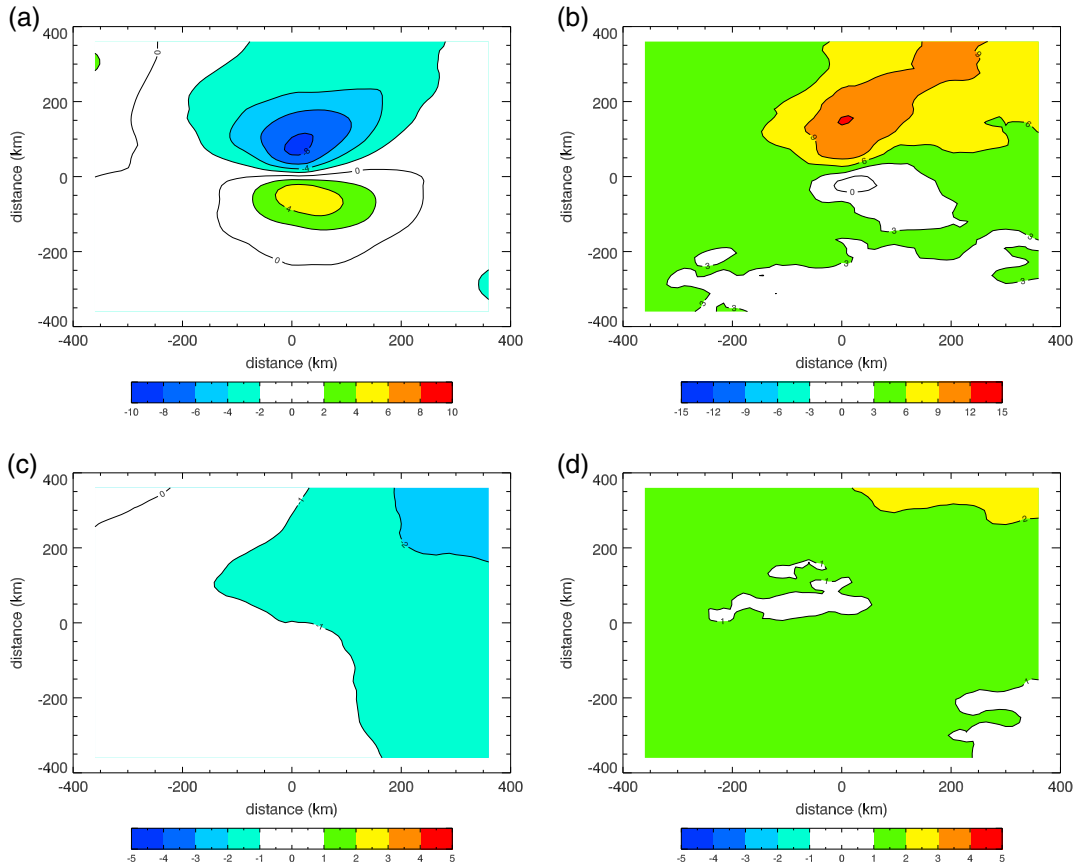
Figure 3. Composites around surface rainfall of (a, c) eddy heat fluxes ($v'\theta'$) and (b, d) cooling by meridional advection ($v \cdot d\theta/dy$). Figures 3a and 3b are for 12kmExp and Figures 3c and 3d for 12kmParam (all at 320 m above the ground). Note different color scales.

become too large across West Africa, with an error of approximately 3 m in the 925 hPa geopotential height, driving too strong a monsoon flow (approximately 9 m by day 2; Figure S9 in the auxiliary material). Similar errors have been diagnosed in other global models and analyses [*Meynadier et al.*, 2010; *Augusti-Panareda et al.*, 2010].

[17] A complete evaluation of the monsoon in each model is beyond the scope of this paper, but Figure 2e shows the observed pressure gradient between Tamanrasset (22.8°N 5.5°E) and Niamey (13.5°N 2.1°E) in 2006 for comparison with *Cascade* and in 2011 for comparison with UM forecasts. These stations are chosen as they are the only two that capture the Sahel-Sahara pressure gradient with sufficient data to resolve the diurnal cycle. They are at a similar longitude, minimizing the effect of the atmospheric tide. The observations and 12kmExp show a strong gradient at 12 UTC and a sustained weak gradient at 18 to 21 UTC, with the diurnal cycle in 12kmExp remarkably close to that observed. The 12kmParam gives too strong a gradient and fails to capture the diurnal cycle, with a relatively weak gradient at 12 to 15 UTC and too strong a gradient by 21 UTC. These errors in 12kmParam are consistent with convective heating over the Sahel occurring too early in the day. The diurnal cycle in errors in 6 hourly UM forecasts is similar to those in 12kmParam: the diurnal cycle is too flat and the model fails to capture the observed strong gradient at 12 UTC, although, overall, the forecast pressure gradient is too weak. These errors in the diurnal cycle are again consistent with the overprediction of convection at midday by

the parameterization (see Text S5 in the auxiliary material). The comparison with wind observations (Text S6 in the auxiliary material) is less clear but weakly supports the hypothesis that explicit convection gives more realistic monsoon winds.

4. Conclusions

[18] We have analyzed *Cascade* simulations, run using the UK Met Office UM, which differ only in their representation of moist convection ("explicit" and "parameterized"), to show that these have fundamentally different representations of the WAM, with important differences occurring as a result of the models' different diurnal cycles in moist convection. For many key aspects, the explicit convection is more realistic than the parameterized one: in particular, it generates more rainfall in the Sahel, with rainfall later in the day. The moist convection is much more similar for the 12 km and 4 km explicit runs than for the 12 km explicit and parameterized runs (consistent with previous work [*Dirmeyer et al.*, 2012; *Pearson et al.*, 2013]).

[19] The main differences between the parameterized and explicit simulations are schematically depicted in Figure 4. The later timing and northward shift of the explicit convection act to weaken the monsoon flow between the Sahel and Sahara and delay its diurnal cycle. The later explicit convection increases surface radiative heating during the day and increases latent heating in the evening, delaying the development of the pressure gradient driving the

(a)

(b)
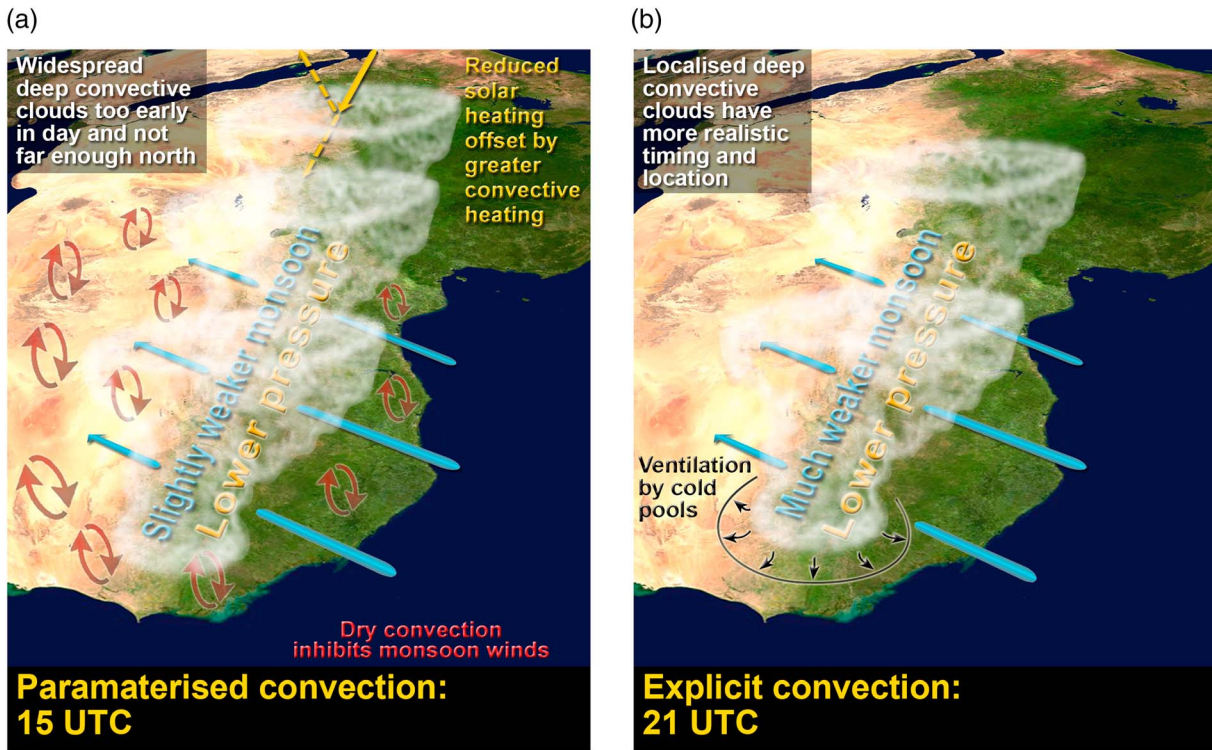
Figure 4. Schematic of how the diurnal cycle of convection impacts the West African monsoon.

monsoon: this gives stronger pressure gradients during the day when boundary layer convection inhibits the monsoon [*Parker et al.*, 2005] and weaker pressure gradients at night when the monsoon flow is maximized. In explicit simulations, storm outflows provide a significant component of the monsoon (consistent with *Garcia-Carreras et al.* [2013]). Since the diurnal timing and more northward location of the explicit convection are more realistic than those of the parameterized, we infer that these interactions between convection and the monsoon are important in reality but poorly captured by the standard parameterized model. Overall, the more realistic explicit convection can be seen as a "governor" to the monsoon: the monsoon not only provides water for moist convection, but moist convection weakens the monsoon.

[20]   The results demonstrate how thermodynamic biases from parameterized convection project upscale to a continental-scale bias in dynamics. An initial comparison with surface pressure observations from two stations in the Sahel and Sahara shows that errors in forecasts from the global UM are consistent with the errors from parameterized convection revealed by the *Cascade* simulations. The location and diurnal cycle in rainfall, and associated cold pools, are a challenge for all global models: our results suggest that parameterizations improving predictions of these aspects of convection will improve not only predictions of rainfall but also predictions of the entire WAM, including Earth system components [*Marsham et al.*, 2011; *Traoré et al.*, 2011].

References

Augusti-Panareda, A., A. Beljaars, C. Cardinali, and I. Genkova (2010), Impacts of assimilating AMMA soundings on ECMWF analyses and forecasts, *Wea. Forecasting*, *25*, 1142–1160.

Biasutti, M., and A. H. Sobel (2009), Delayed Sahel rainfall and global seasonal cycle in a warmer climate, *Geophys. Res. Lett.*, *36*, L23707, doi:10.1029/2009GL041303.

Bock, O., et al. (2011), The large-scale water cycle of the West African monsoon, *Atmos. Sci. Lett.*, *12*, 51–57.

Cook, K. H. (2008), The mysteries of Sahel droughts, *Nat. Geosci.*, *1*, 647–648. doi:10.1038/ngeo320.

Davis, C. A., K. W. Manning, R. E. Carbone, S. B. Trier, and J. D. Tuttle (2003), Coherence of warm-season continental rainfall in numerical weather prediction models, *Mon. Wea. Rev.*, *131*, 2667–2679.

Diongue, A., J. P. Lafore, J. L. Redelsperger, and R. Roca (2002), Numerical study of a Sahelian synoptic weather system: Initiation and mature stages of convection and its interactions with the large-scale dynamics, *Quart. J. Roy. Meteorol. Soc.*, *128*, 1899–1927.

Dirmeyer, P. A., et al. (2012), Simulating the diurnal cycle of rainfall in global climate models: Resolution versus parameterization, *Clim. Dyn.*, *39*, 399–418.

Druyan, L. M. (2011), Studies of 21st-century precipitation trends over West Africa, *Int. J. Climatol.*, *31*, 1415–1424. doi:10.1002/joc.2180.

Emmel, C., P. Knippertz, and O. Schulz (2010), Climatology of convective density currents in the southern foothills of the Atlas Mountains, *J. Geophys. Res. Atmos.*, *115*. doi:10.1029/2009JD012863.

Flamant, C., et al. (2007), Airborne observations of the impact of a convective system on the planetary boundary layer thermodynamics and aerosol distribution in the inter-tropical discontinuity region of the West African monsoon, *Quart. J. Roy. Meteorol. Soc.*, *133*, 1175–1189.

Garcia-Carreras, L., J. H. Marsham, D. J. Parker, C. L. Bain, S. Milton, A. Saci, M. Salah-Ferroudj, B. Ouchene, and R. Washington, (2013), The impact of convective cold pool outflows on model biases in the Sahara, *Geophys. Res. Lett.*, doi:10.1002/grl50239, in press.

Joyce, R. J., J. E. Janowiak, P. A. Arkin, and P. Xie (2004), CMORPH: A method that produces global precipitation estimates from passive microwave and infrared data at high spatial and temporal resolution, *J. Hydromet.*, *5*, 487–503.

Knippertz, P., et al. (2009), Dust mobilization and transport in the northern Sahara during SAMUM 2006—A meteorological overview, *Tellus B*, *61*, 12–31. doi:10.1111/j.1600-0889.2008.00380.x.

Kummerow, C., et al. (2000), The status of the Tropical Rainfall Measuring Mission (TRMM) after two years in orbit, *J. Appl. Meteorol.*, *39*, 1965–1982.

Lean, H. W., et al. (2008), Characteristics of high-resolution versions of the Met Office Unified Model for forecasting convection over the United Kingdom, *Mon. Wea. Rev.*, *136*, 3408–3424.

Marsham, J. H., D. J. Parker, C. M. Grams, C. M. Taylor, and J. M. Haywood (2008), Uplift of Saharan dust south of the inter-tropical discontinuity, *J. Geophys. Res. Atmos.*, *113*. doi:10.1029/2008JD009844.

Marsham, J. H., P. Knippertz, N. S. Dixon, D. J. Parker, and G. M. S. Lister (2011), The importance of the representation of deep convection for modeled dust-generating winds over West Africa during summer, *Geophys. Res. Lett.*, *38*. doi:10.1029/2011GL048368.

Mathon, V., H. Laurent, and T. Lebel (2002), Mesoscale convective system rainfall in the Sahel, *J. Appl. Meteorol.*, *41*, 1081–1092.

Meynadier, R., et al. (2010), West African monsoon water cycle: 2. Assessment of numerical weather prediction water budgets, *J. Geophys. Res. Atmos.*, *115*, doi:10.1029/2010JD013919.

Parker, D. J., et al. (2005), The diurnal cycle of the West African monsoon circulation, *Quart. J. Roy. Meteorol. Soc.*, *131*, 2839–2860.

Pearson, K. J., R. J. Hogan, R. P. Allan, G. M. S. Lister, and C. E. Holloway (2010), Evaluation of the model representation of the evolution of convective systems using satellite observations of outgoing longwave radiation, *J. Geophys. Res.*, *115*. doi:10.1029/2010JD014265.

Pearson, K. J., G. M. S. Lister, C. E. Birch, R. P. Allen, R. J. Hogan, and S. J. Woolnough (2013), Modelling the diurnal cycle of tropical convection across the 'grey-zone', *Quart. J. Roy. Meteorol., Soc.*, ISSN 1477-870X, in press.

Philippon, N., F. J. Doblas-Reyes, and P. M. Ruti (2010), Skill, reproducibility and potential predictability of the West African monsoon in coupled GCMs, *Clim. Dyn.*, *35*, 53–74.

Pohl, B., and H. Douville (2011), Diagnosing GCM errors over West Africa using relaxation experiments. Part I: Summer monsoon climatology and interannual variability, *Cim. Dyn.*, *37*, 1293–1312. doi:10.1007/s00382-010-0911-2.

Randall, D., M. Khairoutdinov, A. Arakawa, and W. Grabowski (2003), Breaking the cloud parameterization deadlock, *Bull. Amer. Meteorol. Soc.*, *84*, 1547–1564.

Redelsperger, J. L., et al. (2002), Multi-scale description of a Sahelian synoptic weather system representative of the West African monsoon, *Quart. J. Roy. Meteorol. Soc.*, *128*, 1229–1257.

Schubert, W. H., P. E. Ciesielski, D. E. Stevens, and H. C. Kuo (1991), Potential vorticity modelling of the ITCZ and the Hadley circulation, *J. Atmos. Sci.*, *48*, 1493–1509.

Solomon, S. D., et al. (eds.) (2007), *Contribution of Working Group I to the Fourth Assessment Report of the Intergovernmental Panel on Climate Change*, Chapter 11, 866–871, Cambridge University Press, Cambridge, United Kingdom and New York, NY, USA.

Stephens, G. L., et al. (2010), Dreary state of precipitation in global models, *J. Geophys. Res. Atmos.*, *115*. doi:10.1029/2010JD014532.

Thorncroft, C. D., and M. Blackburn (1999), Maintenance of the African easterly jet, *Quart. J. Roy. Meteorol. Soc.*, *125*, 763–786.

Thorncroft, C. D., et al. (2003), The JET2000 project—Aircraft observations of the African easterly jet and African easterly waves, *Bull. Amer. Metetorol. Soc.*, *84*, 337–351.

Traoré, S. B., et al. (2011), Characterizing and modeling the diversity of cropping situations under climatic constraints in West Africa, *Atmos. Sci. Lett.*, *12*, 89–95.

Weisman, M. L., W. C. Skamarock, and J. B. Klemp (1997), The resolution dependence of explicitly modeled convective systems, *Mon. Wea. Rev.*, *125*, 527–548.

Xue, Y. K., et al. (2010), Intercomparison and analyses of the climatology of the West African monsoon in the West African Monsoon Modeling and Evaluation project (WAMME) first model intercomparison experiment, *Clim. Dyn.*, *35*, 3–27. doi:10.1007/s00382-010-0778-2.

Yang, G. Y., and J. Slingo (2005), The diurnal cycle in the tropics, *Mon. Wea. Rev.*, *129*, 784–801.

Zhang, C., D. Nolan, C. D. Thorncroft, and H. Nguyen (2008), Shallow meridional circulations in the tropical atmosphere, *J. Clim.*, *21*, 3453–3470.